Heliyon 10 (2024) e37791

Contents lists available at ScienceDirect

Heliyon

journal homepage: www.cell.com/heliyon

Research article

A global view on quantitative proteomic and metabolic analysis of rat livers under different hypoxia protocols

Jin Xu [a], Wen-jie Chen [a], Han-bing Hu [a], Zhi-wei Xie [a], Dong-ge Zhang [a], Jia Zhao [a], Jing Xiang [a], Qi-yu Wei [a], Tawni Tidwell [b], Olivier Girard [c], Fu-hai Ma [d], Zhao-wei Li [a], Yan-ming Ren [a,*]

[a] Qinghai University, Xining, 810001, China
[b] Center for Healthy Minds, University of Wisconsin-Madison, 625 Washington Ave, Madison, WI, 53711, USA
[c] School of Human Sciences (Exercise and Sport Science), The University of Western Australia, Crawley, Western Australia, Australia
[d] Qinghai Institute of Sports Science, Xi Ning, China

ARTICLE INFO

Keywords:
Hypobaric hypoxia
Proteomics
Extreme altitude
Metabolomics

ABSTRACT

Hypobaric hypoxia causes altitude sickness and significantly affects human health. As of now, focusing on rats different proteomic and metabolic changes exposed to different hypoxic times at extreme altitude is blank. Our study integrated *in vivo* experiments with tandem mass tag (TMT)- and gas chromatography time-of-flight (GC-TOF)-based proteomic and metabolomic assessments, respectively. Male Sprague-Dawley rats were exposed to long-term constant hypoxia for 40 days or short-term constant hypoxia for three days, and their responses were compared with those of a normal control group. Post-hypoxia, serum marker assays related to lipid metabolism revealed significant increases in the levels of low-density lipoprotein (LDL), triglycerides (TG), and total cholesterol (TC) in the liver. In contrast, high-density lipoprotein (HDL) levels were upregulated in the long-term constant hypoxia cohorts and were significantly reduced in the short-term constant hypoxia cohorts. Furthermore, metabolic pathway analysis indicated that glycerolipid and glycerophospholipid metabolisms were the most significantly affected pathways in long-term hypoxia group. Subsequently, RT-qPCR analyses were performed to corroborate the key regulatory elements, including macrophage galactose-type lectin (*MGL*) and Fatty Acid Desaturase 2 (*FADS2*). The results of this study provide new information for understanding the effects of different hypobaric hypoxia exposure protocols on protein expression and metabolism in low-altitude animals.

1. Introduction

Hypoxia, predominantly occurring in high-altitude regions, is commonly induced by a deficient oxygen supply, leading to widespread alterations in protein expression across various human tissues [1]. Unacclimatized people traveling to altitudes >2500 m

* Corresponding author.
E-mail addresses: 693633088@qq.com (J. Xu), 2048037676@qq.com (W.-j. Chen), 15202553046@163.com (H.-b. Hu), 137399497@qq.com (Z.-w. Xie), 1435503143@qq.com (D.-g. Zhang), 1735889707@qq.com (J. Zhao), 2227336244@qq.com (J. Xiang), 1060013431@qq.com (Q.-y. Wei), tawni.tidwell@gmail.com (T. Tidwell), olivier.girard@uwa.du.au (O. Girard), gaoxu20172021@163.com (F.-h. Ma), qhdx1290973791@163.com (Z.-w. Li), QH202120212021@163.com (Y.-m. Ren).

https://doi.org/10.1016/j.heliyon.2024.e37791
Received 16 March 2024; Received in revised form 1 August 2024; Accepted 10 September 2024
Available online 12 September 2024

commonly suffer from acute altitude sickness, with symptoms often manifested as follows: headache, gastrointestinal symptoms, fatigue and/or weakness, and dizziness/light-headedness [2]. According to estimates, almost over 500 million humans live at ≥1500 m, 14.4 million at ≥3500 m, although only 0.31 million at ≥5000 m [3]. There are variations in the muscles of professional climbers returning from extremely high altitudes (>5500 m) in terms of mitochondrial volume density, subcellular distribution, oxidative enzyme activity, and protein expression [4].

Gut microbiota-metabolites-neuroendocrine changes in male rats short-term constant exposure to simulated altitude of 5500 m [5], which is closely related to the body's metabolism. At different time (1–12 weeks) of exposure to hypobaric hypoxia at an altitude of 5500 m, the secretion of atrial natriuretic peptide and brain natriuretic peptide in rats will change, which is involved in cardiovascular homeostasis [6]. Long-term hypoxia may lead to metabolic alterations including diminished mitochondrial function and enhanced glycolysis. Hypoxia-inducible factor 1α (HIF-1α) plays a central role in regulating hepatic lipid metabolism. The expression of HIF-1α in the liver promotes lipid uptake and synthesis while decreasing lipid oxidation, consequently ultimately contributing to hepatic steatosis [7]. Increased expression of HIF-1α in the liver and serum under hypoxic conditions has been found [8,9]. In individuals with cardiorespiratory illnesses, short-term constant hypoxia diminishes the synthesis of the cytochrome P450 subfamily members, thereby increasing the risk of heart failure. Short-term hypoxia exposure may hinder the P450 subfamilies in the liver from metabolising medications, thus, potentially posing a risk to patients.

The liver plays a pivotal role in most physiological processes and is essential for maintaining homeostasis. Recognised for its critical function in metabolising glucose, glycogen, and lipids, the liver provides energy-generating fuels to the adjacent tissues, thereby ensuring stability under extreme altitude conditions.

Maladaptation caused by long-term constant hypoxia is closely linked to the liver metabolic status [10]. For instance, long-term constant hypoxia is associated with the pathogenesis of nonalcoholic steatohepatitis (NASH), which is a prevalent liver disease. Nonalcoholic fatty liver disease (NAFLD) is thought to contribute to the progression of NASH, with alterations in lipid metabolism induced by short-term constant hypoxia linked to the activation of key enzymes and metabolic pathways. This suggests that oxidative stress and lipid peroxidation are critical factors that modulate NAFLD.

Tandem mass tag (TMT)-based proteomic analysis involves labelling all proteins expressed in a genome or complex mixture. For TMT-based proteomics investigations on adaptation to high-altitude hypobaric hypoxia exposure, plasma proteome profiles and differentially expressed proteins have been reported in people at high and low altitudes [8], and plasma proteomic changes have also been found in people exposed to different hypoxia time [11]. Wang et al. identified 19 differential proteins that play an important role in the occurrence and development of high-altitude polycythemia (HAPC) in plasma samples from HAPC patients and healthy controls [12]. In addition, hypoxia-related changes in the proteins expression of rats for 35 days have been observed in our previous study [13].

Metabolomics is also widely used in the study of high altitude. Metabolomics has played an important role in the study of urine biomarkers of rats under hypobaric hypoxia [14]. Further, urinary metabolites of humans that may be used to identify acute mountain sickness susceptible subjects have been reported through the use of metabolomics [15]. Differential metabolites in serum that can be used as early warning indicators of acute injury are found under conditions of high altitude hypoxic exposure [16]. Based on the above studies, we hypothesized that there may be differences in expressed proteins and metabolites in rats after hypoxia.

Compared to our previous study using only proteomics and a single long-term hypoxia protocol (a consecutive hypoxia for 35 days),

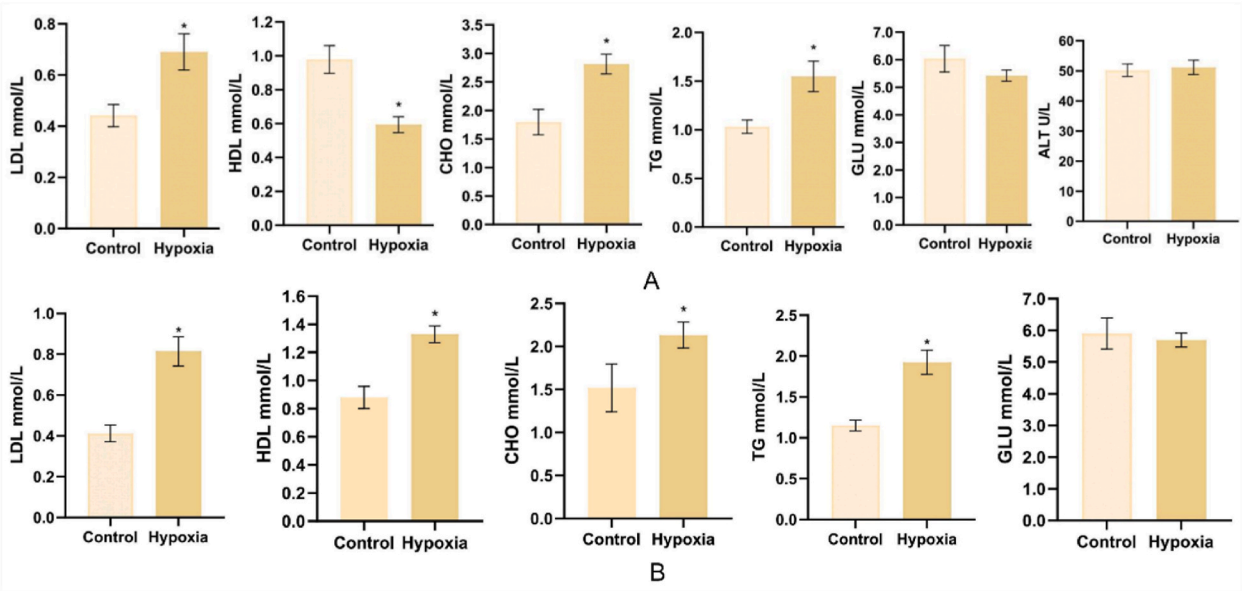

Fig. 1. Plasma lipid metabolism profiles. Serum levels of LDL, HDL, TG, CHO, GLU (n = 8). (A)Short-term hypoxia group vs normoxia. (B)Long-term hypoxia group vs normoxia * $P < 0.05$.

in this study, we combined animal experiments under different hypoxia protocols with TMT-based proteomic analysis and metabolomic profiling to elucidate the metabolic alterations caused by oxygen condition at extreme altitude. Therefore, this study will be more comprehensive and our findings revealed that hypoxia induced metabolic pathway alterations in the liver based on changes in metabolites and expressed proteins. This will provide a scientific basis for confirming biomarkers for hypobaric hypoxia-induced diseases and understanding of the effects of hypoxia on metabolic pathways alterations in future human studies, although there are some differences between these animal data and human metabolic results.

2. Results

2.1. Plasma lipid metabolism profiles and basic information

A Comprehensive analysis of metabolic markers and serum lipids in the short-term and long-term hypoxia groups was performed on Day 3 and Day 40, respectively. As widely used liver enzyme, alanine aminotransferase (ALT) is a direct indication of liver health. On the other hand, the blood glucose (GLU) test, reflects the glucose level at the moment of sampling and is mainly used for the diagnosis of diabetes mellitus and to rule out the possibility of diabetes. Under different hypoxic conditions, our analysis using instruments chemie (Delfzijl, the Netherlands) kits found no significant changes in serum ALT or GLU levels. Moreover, TG, TC, and LDL levels were higher in the hypoxic group than in the normoxic group ($P < 0.05$) (Fig. 1). Conversely, the HDL levels in the short-term hypoxia group showed a different pattern from those in the long-term constant hypoxia group (Fig. 1A,B). In particular, LDL levels were approximately doubled in the long-term constant hypoxia group compared to the normoxic group (Fig. 1B). The effects of 40-day hypobaric hypoxia on rat well being, food and water intake, body weight, and ALT are shown in Table 1. These findings suggest that hypoxia may significantly influence lipid and glucose metabolism.

2.2. HE staining of liver tissue

HE staining of right lobe of rat liver tissue in each group was observed under a microscope (400 × magnification) on Day 3 and Day 40 (Fig. 2). In the control group, normal liver cell morphology was observed, with no morphological changes of the central vein or hepatic sinusoids. In the hypoxic group, the volume of hepatocytes increased and many vacuoles of different sizes appeared in the cytoplasm under the use of a micrometer; however, the nuclear structure remained normal and neither the central veins nor the hepatic sinus were dilated or contracted.

2.3. Rat liver metabolomics analysis

2.3.1. Rat liver metabolomics profiles from GC-TOF/MS data analysis

Principal component analysis (PCA) was conducted on the GC-TOF spectra of liver samples obtained from animals subjected to hypoxic and normoxic conditions (Fig. 3A and B). The PC score graphs exhibited a distinct segregation from those of the short-term and long-term constant hypoxic, and normoxic groups. Orthogonal Partial Least Squares Discriminant Analysis (OPLS-DA) (Fig. 3C,D) and OPLS-DA permutation plots were used to identify the most distinctive variables defining grouping patterns. In the short-term constant hypoxia group, R2Y was found to be 0.89 with a Q2 intercept of −0.45, and the majority of R2 and Q2 values on the right side exceeded those on the left side. Furthermore, Q2 intersects with the negative y-axis, thereby indicating that the model is reliable and free of overfitting. When R2 exceeds 0 and Q2 is below 0, the model is not subject to overfitting, and is deemed reliable [10]. The quality parameters of the OPLS-DA model suggested that the first seven components constituted the most effective cluster classification (Fig. S1A). Additionally, the long-term constant hypoxia groups exhibited favourable model quality characteristics in the OPLS-DA analysis, with R2 and Q2 values of 0.88 and −0.48, respectively. These values indicated that the first seven components were the most effective in classifying the clusters (Fig. S1B). Volcano plots were constructed to identify significantly upregulated and downregulated metabolites that defined the clustering patterns (Fig. 3E and F).

2.3.2. Identification of the metabolites

A number of differentially expressed liver metabolites were selected using the criteria of VIP >1.0 and P-value<0.05. In the short-term hypoxia group, 34 significantly altered metabolites were found, of which 17 had elevating levels, such as cortisone, pantothenic acid, and 3-hydroxybutanoic acid, and 17 had decreasing levels, such as L-threose 2, oxalacetic acid, and sorbose 2 (Table S1A). In the

Table 1
Comparison of rats under long-term hypoxia versus normoxia on Day 40.

Variables	Normoxia (n = 8)	Long-term hypoxia (n = 8)	*p*-values
Well-being[a]	+	–	
Food intake (g)	49.38 ± 1.98	47.98 ± 1.18	0.25
Water intake (mL)	37.0 ± 1.5	8.5 ± 0.7	<0.001
Body weight (g)	388.98 ± 15.53	189.39 ± 6.87	<0.001
ALT (U/L)	53.48 ± 1.82	54.57 ± 3.95	0.34

[a] Liver histological evaluation was used to assess the health of the rats. +: healthy, -: obvious histological changes.

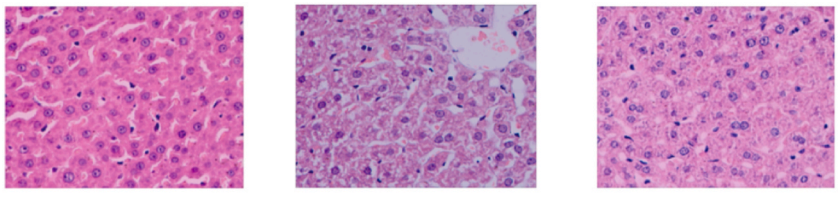

Fig. 2. HE staining of liver tissue (magnification 400×). This analysis revealed changes in the volume of hepatocytes, the presence of vacuoles in the cytoplasm. (A) Normoxia (B) Short-term hypoxia (C) Long-term hypoxia.

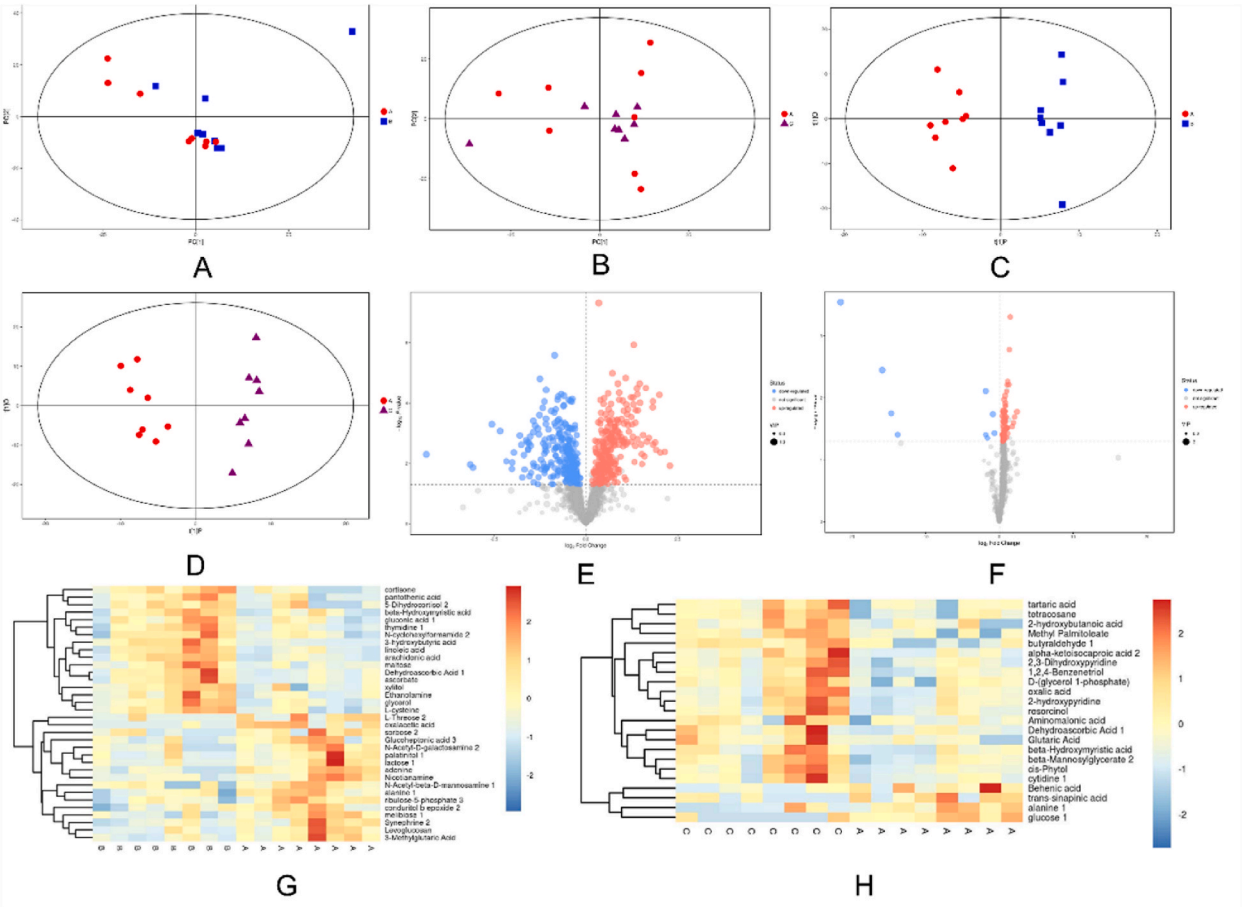

Fig. 3. Effect of hypobaric hypoxia on differential metabolites in rat livers (n = 8)
(A) PCA score scatter plot of normoxia vs short-term hypoxia. (B) PCA score scatter plot of normoxia vs long-term hypoxia (C) The OPLS-DA statistical analysis of normoxia vs short-term hypoxia (D) The OPLS-DA statistical analysis of normoxia vs long-term hypoxia (E) Volcano plot of significant metabolites between short-term constant hypoxia and normal groups. (F) Volcano plot of significant metabolites between long-term constant hypoxia and normal groups. (G) The top 34 significantly up/down regulated metabolites in heatmap of short-term hypoxia group. (H) The top 23 significantly up/down regulated metabolites in heatmap of long-term hypoxia.

long-term hypoxia group, 23 significantly altered metabolites were found, of which behenic acid, trans-sinapinic acid, alanine 1, and glucose 1 levels were downregulated and 19 metabolites, such as tartaric acid, glutaric acid, and 2-hydroxybutanoic acid were upregulated (Table S1B). The heatmap distinctly illustrates the top 34 and 23 significantly upregulated and downregulated metabolites in the short-term (Fig. 3G) and long-term hypoxia groups (Fig. 3H), respectively.

2.4. Rat liver proteomics analysis

2.4.1. Differentially expressed proteins

To study the differences in liver proteins between the hypoxic and normoxia groups, we performed the analysis by TMT. The number of identified proteins was 5740 (Table S2A). To screen differential proteins, the standard was set as fold change≥1.5 or fold change≤2/3. A total of 130 and 183 differentially expressed proteins were identified in the short-term and long-term hypoxia group, respectively(Tables S2B and 2C). Among the 130 differential proteins, 77 proteins were significantly up-regulated and 53 proteins were significantly down-regulated. Among the 183 differential proteins, 128 were significantly up-regulated and 55 were significantly down-regulated. These results suggest that hypobaric hypoxia has an effect on liver protein expression.

2.4.2. Gene ontology (GO) enrichment analysis of differentially expressed proteins

We performed a GO analysis to explore the potential roles of the differentially expressed proteins following exposure to constant hypoxic conditions. The analysis revealed the presence of several cellular components, including extracellular regions, membrane-enclosed lumens, macromolecular complexes, and cell junctions (Fig. 4). Concerning molecular functions, our analysis identified enriched categories including catalytic activity, binding, transporter activity, and antioxidant activity (Fig. 4). The identified enriched biological processes included cellular processes, single-organism processes, biological regulation, metabolic processes, and developmental processes (Fig. 4). These findings suggest that constant hypoxia significantly affects metabolic processes and elicits responses to hypoxic stimuli in the rat liver.

2.4.3. Co-expression network analysis of differential expressed proteins

Through weighted gene co-expression network analysis of bioinformatics analysis, we plotted gene co-expression network and core genes. Fig. S2 illustrates the co-expression network of proteins in rat livers that exhibited significant differential expression following hypoxia. The primary proteins identified include solute carrier family 24 member 1 *(SLC24A1)*, aldehyde dehydrogenase 2 *(ALDH2)*, ATP-citrate lyase *(ACLY)*, acetyl-Coenzyme A carboxylase beta *(ACACB)*, aldo-keto reductase 1C3 *(AKR1C3)*, cytochrome P450 family 1 subfamily A member 1 *(CYP1A1)*, cytochrome P450 family 1 subfamily A member 2 *(CYP1A2)*, cytochrome P450, family 4, subfamily A, polypeptide 8 *(CYP4A8)*, acyl-CoA synthetase medium-chain family member 2 *(ACSM2)*, ras-associated protein 1 *(RAP1A)*,

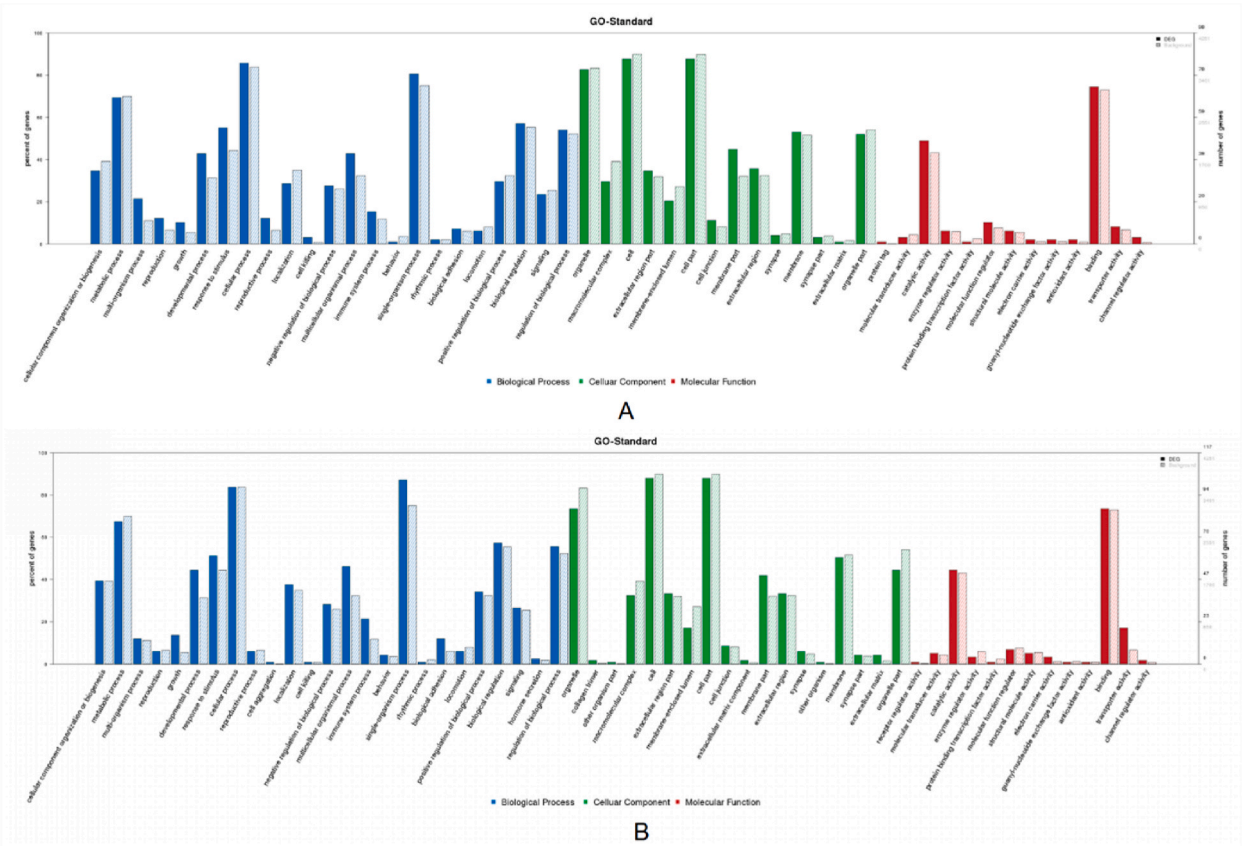

Fig. 4. GO-Standard. GO analysis revealed the presence of genes significantly enriched in specific cell components, molecular functions or biological processes during hypoxia. (A) Between short-term hypoxia and normoxia groups. (B) Between long-term hypoxia and normoxia groups.

interferon-stimulated Gene 15 *(ISG15)*, phosphoglycerate dehydrogenase *(PHGDH)*, 17β-hydroxysteroid dehydrogenase 2 *(HSD17B2)*, and arachidonic acid 15-lipoxygenase-1 *(ALOX15)*. These proteins play critical roles in fatty acid metabolism.

2.5. Pathway analysis

We conducted Kyoto Encyclopedia of Genes and Genomes (KEGG) analysis, pathway analysis, KEGG-pathway enrichment, and GO enrichment of bioinformatics analysis to enhance our understanding of the intracellular pathways affected by hypobaric hypoxia. In the KEGG-pathway enrichment analysis of proteomics, both steroid hormone biosynthesis, linoleic acid metabolism, and arachidonic acid metabolism of the two hypoxic groups were confirmed (Fig. 5A and B). This is partially consistent with the results of pathway analysis (Table S3A) and KEGG analysis (Table S4A) of metabolomics in the short-term hypoxia group. In the short-term hypoxia group, ascorbate and aldarate metabolism confirmed(Fig. 5A) were also identified in KEGG analysis of metabolomics (Table S4A). Unsaturated fatty acid metabolic process was determined in GO enrichment analysis of proteomics (Fig. S3A) and pathway analysis of metabolomics (Table S3A). In addition, the regulation of lipolysis in adipocytes and ABC transporters confirmed in the long-term hypoxia (Fig. 5B) were reconfirmed in the KEGG analysis of the metabolomics (Table S4B).

By KEGG analysis of metabolomics, differential metabolites in the short-term and long-term hypoxia groups were labeled in the metabolic pathway, especially retinol metabolism and chemical carcinogenesis were confirmed in both groups (Fig. 5C and D). Based on the metabolic pathway analysis, in short-term constant hypoxia group, linoleic acid metabolism was most affected by metabolic

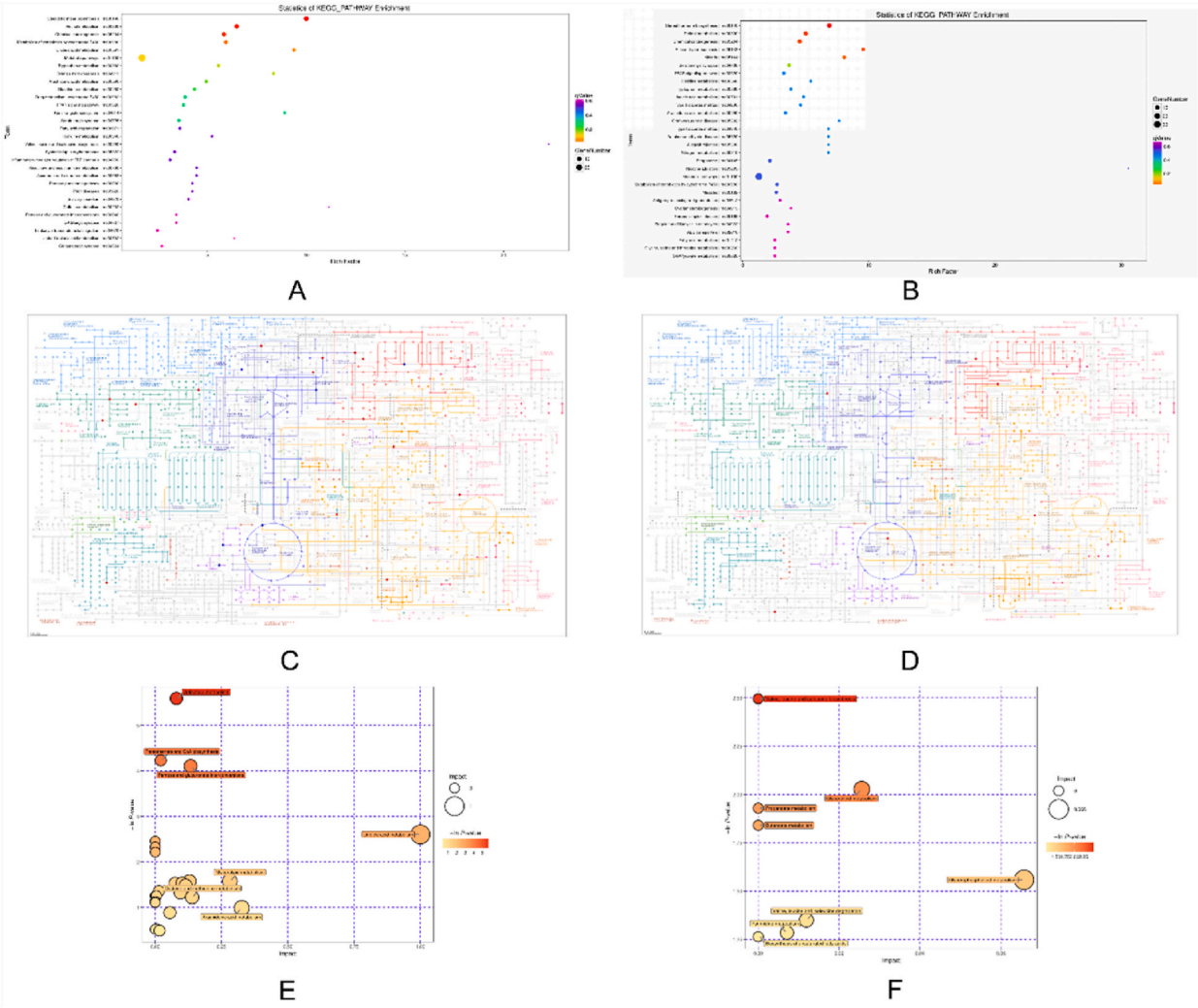

Fig. 5. Pathway analysis. (A)KEGG-pathway analysis of short-term hypoxia vs normoxia. (B) KEGG-pathway analysis of long-term hypoxia vs normoxia. (C) Metabolic pathways with red(up-regulated)/blue (down-regulated) dots representing the differentially expressed compounds of short-term hypoxia vs normoxia. (D) Metabolic pathways with red(up-regulated)/blue (down-regulated) dots representing the differentially expressed compounds of long-term hypoxia vs normoxia. (E) Metabolic pathway analysis bubble plot of short-term hypoxia vs normoxia. (F) Metabolic pathway analysis bubble plot of long-term hypoxia vs normoxia.

pathway analysis (Fig. 5E).

Correspondingly, it was evident that the glycerolipid and glycerophospholipid metabolism pathways were the most significantly affected in long-term hypoxia group (Fig. 5F).

Through GO enrichment analysis of proteomics, we identified the top 30 biological processes in the short-term hypoxia group and the long-term hypoxia group, respectively (Fig. S3). Through our analysis of the proteomics data, we identified protein precursors that play significant roles in many metabolic pathways, including fatty acid degradation and histidine metabolism in short-term hypoxia group (Fig. 5A) and fatty acid metabolism in long-term hypoxia group (Fig. 5B). These findings indicate that hypobaric hypoxia has a major impact on pathways in rat livers.

2.6. Verification of differentially expressed proteins between control and hypoxic samples using real-time quantitative polymerase chain reaction (RT-qPCR)

To verify the quantitative data obtained by TMT proteomics, RT-qPCR was performed. The selection criteria of genes were: a) up- or down-regulation in all replicate analyses of proteomics; and b) associated with metabolic pathways; and c) potential as a biomarker after hypoxic exposure at high altitude. In the short-term constant group, Fig. 6A illustrates the gene expression levels of Fatty Acid Desaturase 2 (*FADS2*), Angiopoetin-like 4 (*ANGPTL4*), Solute Carrier Family 24 Member 1 (*SLC24A1*), Acyl-CoA Synthetase Medium Chain Family Member 2 (*ACSM2*), Cytochrome P450 Family 1 Subfamily A Member 1 (*CYP1A1*), and Cytochrome P450 Family 1 Subfamily A Member 2 (*CYP1A2*). In the long-term constant hypoxia group, adipose triglyceride lipase (*ATGL*), macrophage galactose-type lectin (*MGL*), long-chain acyl-CoA synthetase (*ACSL*), glycerol-3-phosphate acyltransferases (*GPAT*), and purple acid phosphatase (*PAP*) were selected to validate the proteomics results (Fig. 6B). These findings are consistent with those of proteomic analysis. The reference gene against which expression was measured is *GAPDH*.

3. Discussion

Recently, a TMT-liquid chromatography-tandem mass spectrometry (LC-MS/MS) method was developed for the identification and quantification of proteins. Yu et al. [17] revealed diabetic foot ulcer pathogenesis and potential therapeutic targets by TMT-based serum proteomic profiling. Xia et al. [18] employed TMT label-based proteomics to identify protein differences in the cerebral cortex of TauT-knockout rats. Consequently, systematic screening of deregulated proteins could provide profound insights into the molecular mechanisms underlying the responses to stimuli.

Frequent exposure to high altitudes often leads to hypoxia. Zhao's study on the adaptation of Tibetan sheep lungs to high-altitude hypoxia using proteomic sequencing revealed key proteins and pathways related to gas transport, oxidative stress, and angiogenesis [19]. The results linked to these proteins and pathways concurred with those of the physiological studies, thereby corroborating the physiological findings reported by Zhao.

Metabolomics, emerging from proteomics, enables the identification of small-molecule metabolites and reflects changes in endogenous metabolites during progression. Chen et al. [20] demonstrated that prolonged intermittent (O_2 from 21 % to 6 %,for 8 h

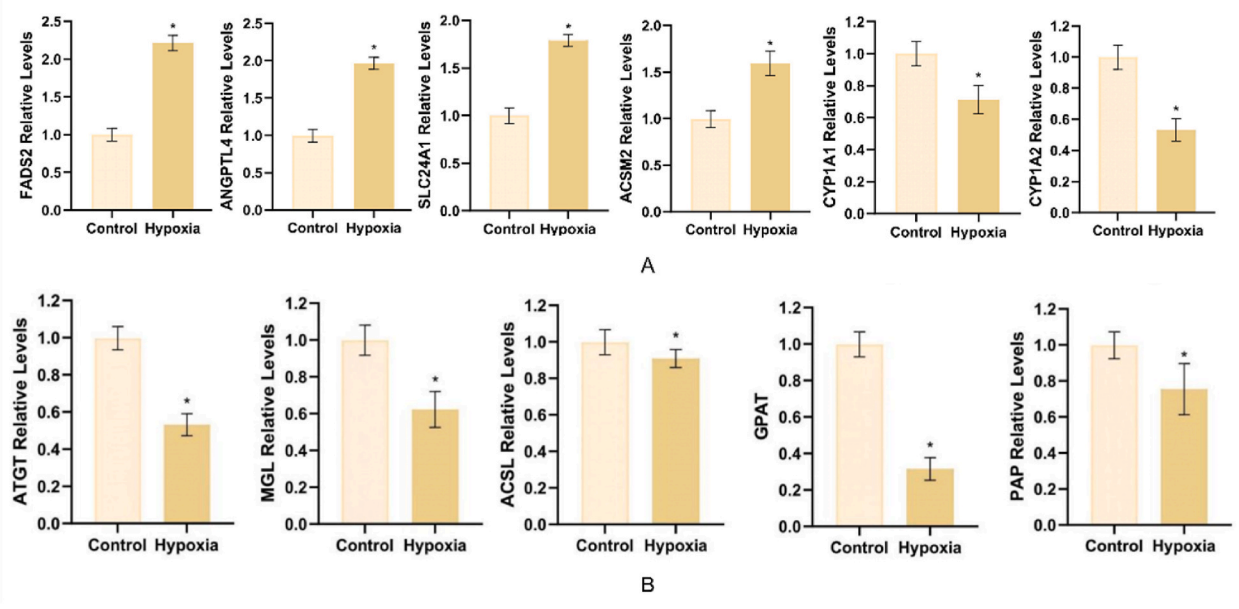

Fig. 6. Verification of differentially expressed proteins by RT-qPCR (n=8). (A) The control vs short-term hypoxia group. (B) The control vs long-term hypoxia group (*$P < 0.05$).

per day, lasted 12 weeks) hypoxia induces significant changes in lipid metabolism in the mouse liver, thereby leading to extensive liver damage. Yan et al. [21] discovered that obese rats exhibited a significant increase in serum free fatty acid (FFA) and myocardial TG levels upon exposure to long-term constant persistent (O_2 14 %, 4 weeks) hypoxia at an altitude of 4300 m for eight weeks.

The liver is crucial for maintaining homeostasis and regulating metabolism. These processes require a significant amount of oxygen, which makes the liver highly sensitive to hypoxic conditions. It can be inferred that hypoxic conditions prompt changes in hepatic metabolism, particularly affecting lipid metabolism. The findings and insights inspired the design and execution of the present investigation.

In this study, our investigation revealed no significant changes in ALT or GLU levels under hypoxic conditions ($P < 0.05$). Similarly, Song et al. [22] observed no significant differences in GLU levels between normoxic and long-term high-altitude exposure groups (at 4300 m with O_2 14 % for eight weeks). Thomas et al. [23] showed that whole-body glucose tolerance, initially triggered by long-term intermittent hypoxia (2 weeks, 1-min cycle, fraction of inspired oxygen 21–5%, 8 h/day), was effectively counteracted.

In this study, GC-TOF metabolomics was used to explore liver metabolism under hypoxic conditions that are common at high altitudes. Specifically, we utilised advanced pattern recognition techniques, including PCA and OPLS-DA analysis, which revealed a clear distinction between hypoxia-exposed and normoxic control groups. Essential metabolites were analysed to explore metabolic pathways, revealing several key pathways related to lipid metabolism: glycerolipid metabolism, glycerophospholipid metabolism, and the regulation of lipolysis. Krishnan et al. [24] found that hypoxia induces FFA uptake and glycerin biosynthesis by activating peroxisome proliferator-activated receptor (PPAR), leading to cardiac steatosis. Consistent with our findings, Liao et al. [25] reported that glycerophospholipid content was 7.03-fold higher in hypoxic conditions. Systemic metabolic homeostasis preservation is partly achieved through lipolysis modulation, which is controlled by a complex regulatory network [26]. In groups exposed to long-term hypoxia, as an integral part of the glycerolipid/free fatty acid (GL/FFA) cycle [27], examination of differentially expressed proteins and differential metabolites by KEGG analysis revealed that the regulation of lipolysis in adipocytes was enriched, which is consistent with enhanced lipolysis of 3T3-L1 cells under hypoxia [28]. We hypothesized that these pathways contribute significantly to changes in liver metabolism, as exemplified by increased alanine levels in rats subjected to hypoxia.

Oxaloacetate and malic acid are considered to be the end products of the tricarboxylic acid cycle [29]. In the short-term hypoxia group, a significant down-regulation of oxaloacetate may imply a reduction in levels of tricarboxylic acid (TCA) cycle in rats to some extent. In the long-term hypoxia group, glutaric acid, a precursor of α-ketoglutarate, was significantly increased compared with the normoxia group, and no significant changes in oxaloacetate and malic acid were found. In addition, 2-hydroxybutyrate has been shown to stimulate the expression of lipid-degrading proteins in hepatocytes and inhibit oleic acid-induced triglyceride accumulation [30]. In this study, we found that 3-hydroxybutyrate, which is precursor of 2-hydroxybutyrate, and 2-hydroxybutyrate, were identified to be significantly elevated in the short-term and long-term hypoxia groups, respectively. Therefore, we hypothesized that rats may be as resistant to long-term hypoxia-induced lipid metabolism disorders as possible through the transformation of differential metabolites.

We validated pecific genes that play crucial roles in lipid metabolism under various hypoxic conditions. Based on the results of the proteomics, in the long-term hypoxia group (Fig. 6B), we investigated the GL/FFA cycle by measuring *MGL, ACSL, and GPAT* levels, which in turn alter lipid metabolism [25]. *MGL*, *ACSL*, and *GPAT* levels were downregulated in the long-term hypoxia exposure group. *MGL* encodes a serine hydrolase belonging to the AB hydrolase superfamily and its main function is to facilitate the transformation of monoacylglycerides into free fatty acids and glycerol. Although *MGL* regulates the levels of fatty acids that serve as signalling molecules, it can potentially be inhibited by hypoxic exposure [31]. *ACSL* catalyse the activation of long-chain fatty acids, thereby enabling their utilisation in the production of cellular lipids and breakdown through beta-oxidation. This process is necessary for the integration of fatty acids into phosphatidylcholine. Triacylglycerol (TAG) synthesis is initiated by sequential acylation of glycerol-3-phosphate by *GPAT*, which results in the formation of lysophosphatidic acid. Subsequently, the lysophosphatidic acid undergoes further esterification and transformation to phosphatidic acid [32]. Overall, *MGL, ACSL*, and *GPAT* are all related to glycerolipid metabolism. Our unique observations indicated that these variables were all downregulated after 40 days of hypoxic exposure. We speculate that the GL/FFA cycle is partially inhibited after 40 days of long-term hypoxic exposure, which might be involved in lipometabolic disorders.

In the short-term hypoxia constant hypoxia group, the levels of *CYP1A1* and *CYP1A2*, both of which encode the cytochrome P450 superfamily of enzymes, were significantly downregulated. Short-term mild hypoxia lowers the overall content and activity of P450, as well as the *in vivo* expression of *CYP1A1* and *CYP1A2* [33]. Cytochrome P450 proteins function as monooxygenases, and facilitate many processes involved in drug metabolism as well as the creation of cholesterol, steroids, and other lipids. These findings were confirmed by qPCR (Fig. 6). The levels of *FADS and ANGPTL4* were upregulated in the livers of the short-term hypoxia group compared to the control group. *FADS2* belongs to the gene family of fatty acid desaturases, which encode delta-6 desaturases (*D6D*), essential enzymes in the production of long chain polyunsaturated fatty acids (*LC-PUFA)* that regulate glucose and lipid metabolism in animals [34]. ANGPTL4 is a secreted glycoprotein that is activated by peroxisome proliferator-activated receptors and plays a pivotal role in the physiological regulation of lipid and glucose metabolism [35]. In summary, the genes mentioned above exhibited a significant correlation with metabolic pathways critical for oxidative stress, thus, providing invaluable insights and laying a solid groundwork for subsequent research.

Disruption of hepatic oxygen homeostasis is associated with the aetiology of a broad range of liver diseases [36].In line with our findings, hypoxia and HIF-1α strongly stimulate the production of hypoxia-inducible lipid droplet-associated (HILPDA) [37], and in mice with severe liver disease such as NASH, HILPDA deficiency slightly reduces liver triglyceride storage [38], suggesting hypoxia can affect lipid distribution in hepatocytes.

It should be noted that the occurrence and severity of hypoxic responses in rats are known to vary significantly within populations, with two opposite extreme phenotypes–high resistance (HR) and low resistance (LR) to hypoxia [39]. Mironova et al. [40] found that

in the cerebral cortex of LR rats, the number of mitochondria, which are tiny electron-dense, increased about threefold. Conversely, after this hypoxia exposure, the number of tiny mitochondria in the cerebral cortex of HR rats remained almost constant and remained significantly higher than that of control LR rats. Mironova et al. [41] also analyze the mitochondrial ATP-dependent K^+ transport systems in rats with varying levels of short-term constant hypobaric hypoxia tolerance. Using NADH-dependent respiratory substrates, it was discovered that the HR rats had an ATP-dependent swelling rate 50–75 % higher than the LR animals. This suggests that the initial difference in hypoxic tolerance will result in different responses in rats under different hypoxia exposure treatments. At the same time, given the intricate mechanisms and pathways involved in liver metabolism, the precise regulatory mechanisms warrant extensive research for comprehensive elucidation.

Our study demonstrated that hypoxia induces wide metabolic alterations in the liver. In response to hypoxia, rats maintained normal physical activity by downregulating biosynthetic processes, thereby reducing their energy expenditure. This will also provide a basis for research on specific issues that are common for the general population in plains to travel to extreme altitudes, such as the length of stay.

4. Methods

4.1. Animals and treatment

Following a one-week acclimatization period during which the rats were fed a standard diet, they were subjected to constant hypoxic conditions. An *in vivo* experiment was performed according to previously reported methodologies [21]. Male Sprague-Dawley rats were randomly assigned into three distinct groups (n = 8/group): normal group, the rats were exposed to normoxia; two hypoxia protocols were used, one group was subjected to long-term hypoxia for a continuous 40-day period while the other group experienced acute hypoxia for a 3-day period. Both hypoxic groups were subjected to hypobaric hypoxia at an altitude of 5500 m (380 mmHg). This was achieved using an FLYDWC50-1C low-pressure hypoxic experimental chamber (Guizhou Fenglei Air Ordinance LTD, Guizhou, China). Rats were housed under controlled environmental conditions: a stable temperature of 25 ± 2 °C, humidity of 50 ± 10 % and a consistent 12-h light/dark cycle. Rats are placed in rearing cages with regularly changed normal laboratory diet and sterilised water, while the cages are located in low-pressure oxygen chamber. On the final day, the rats were euthanised, and their blood and liver tissues were collected and subsequently stored at −80 °C. Sodium citrate was employed as anticoagulants. In this research, no deaths occurred in the rats. This study was reviewed and approved by the Ethics Committee of Medical Ethics Committee of Qinghai University School of Medicine with the approval number: 2019-ZJ-876. The work described has been carried out in accordance with the U. K. Animals (Scientific Procedures) Act, 1986. All animal studies comply with the ARRIVE guidelines.

4.2. Plasma lipid metabolism profiles

The Vitros DT60 II Chemistry System (Johnson & Johnson, Minnesota, USA) was used to enzymatically measure total cholesterol levels. Lipoprotein particles were separated with a SMART LC system (Pharmacia Biotech, Uppsala, Sweden) using a Superose-6 column, which facilitated the measurement of LDL and HDL levels. Liver samples were homogenised with a Stir-Pak® (Barrington, IL). Triglyceride levels in the liver were quantified using a kit (Instruchemistry, Delfzijl, Netherlands).

4.3. HE staining

The right lobe of rat liver was fixed in 4 % paraformaldehyde for 24 h, embedded in paraffin, and cut into 4 μm-thick slices for HE staining. The slices were baked at 60 °C overnight, then dewaxed with xylene and soaked in ethanol at various levels: xylene for 10 min; xylene for 10 min; anhydrous ethanol for 5 min; 95 % ethanol for 5 min; 80 % ethanol for 5 min; 75 % ethanol for 5 min; distilled water for 2 min. Then the slices were stained with haematoxylin for 10 min, rinsed with tap water until there was no foam, fractionated with 1 % hydrochloric acid alcohol for 1 s, and rinsed with tap water for 5 min, rinsed with tap water for 5 min, and stained with eosin for 2 min at room temperature. Subsequently, gradient dehydration, transparency and sealing was carried out as follows: 50 % ethanol for 2 min; 75 % ethanol for 2 min; 95 % ethanol for 2 min; 95 % ethanol for 2 min; anhydrous ethanol for 2 min; anhydrous ethanol for 2 min; mixed solution of xylene and anhydrous ethanol (1:1) for 1 min; and xylene for 2 min. Neutral gum was used to seal the slices. Finally, 40 × and 400 × ultra-structures of liver tissues were observed using light microscopy, and the results were analysed and photographed. Ten high magnification fields (× 400) were observed for each animal.

4.4. The metabolomics analysis of rat liver samples

4.4.1. GC-TOF spectroscopic analysis

In the case of groups exposed to long-term oxygen deprivation, liver samples were preserved by freezing and then combined with 200 lL of deuterated 0.2M sodium phosphate buffer (with a pH of 7.4) that included 1 mM TSP in D_2O. TSP was used as a chemical shift reference (d = 0) and D_2O was used as a lock solvent. The samples were centrifuged at 5000 rpm for 5 min to remove particulate matter. The supernatant was transferred to a sample tube. The GC-TOF spectra were obtained using a Bruker Avance III spectrometer (Bruker, Germany) equipped with a Bruker probe operating at 600 MHz and 298 K. A standard one-dimensional water pre-saturation pulse sequence (NOESYPR1D) was used to suppress the water signals.

A total of 192 scans were conducted, each lasting 1.7 s, and split into 64,000 data points across a9615.4 Hz spectral width. A 2-s

relaxation delay was observed between the scans. Raw FIDs were processed with an exponential function by applying 0.3 Hz line broadening, followed by fast Fourier transformation. GC-TOF spectra from each sample were subjected to phase and baseline correction using a Bruker Topspin 2.1 (Bruker, Germany). The TSP reference peak was set to d = 0. The spectra of normoxic and hypoxic groups were visually inspected.

4.4.2. Data reduction and pattern recognition (PR) analysis

Following phase and baseline corrections, the GC-TOF spectra underwent additional adjustment to account for pH-dependent peak shifts using the icoshift (Interval Correlation Optimized Shifting) technique. Icoshift is a software tool that corrects spectral misalignments through an insertion/deletion model while adjusting the spectral intervals. It utilises fast Fourier transformation for the quick alignment of extensive GC-TOF datasets in seconds. Spectra were binned from d = 0.2–10 ppm using an optimized bucketing algorithm (OBA) with a 0.01 ppm bucket width and 50 % slackness. The OBA adjusts the bucket sizes by finding the lowest data points to set the bucket borders based on the averaged GC-TOF spectra. Slackness allows border adjustments to determine the local minima in the spectrum. Regions containing urea (5.2–6.2 ppm) and water (4.2–5.2 ppm) were excluded from binning.

The binned data were analysed using MetaboAnalyst 3.0. Normalisation and scaling used the sum of intensities and Pareto scaling, respectively, followed by a PR analysis. Liver metabolic profiles were analysed using PCA and OPLS-DA to identify similarities or differences. PCA is an unsupervised method that reduces complex data to principal components (PCs) with PCA score plots analysed for class-independent clusters. OPLS-DA, a supervised PR method, modelled spectral and class information links with its score plots examined for class-dependent clusters. The concentrations of polar metabolites (specifically, the top 25 significant buckets) in animal livers before and after exposure were calculated by manually integrating individual peaks and normalising them against the total spectra. These concentrations were visualised using box-and-whisker plots. Normalised concentrations were used for metabolic pathway analysis to evaluate the changes in response to hypoxia. Metabolic pathway analyses were performed using MetaboAnalyst 2.0 online. The metabolic pathway analysis employed a rat (*Rattus norvegicus*) pathway library, global testing, and out-degree centrality algorithms, thereby yielding fit factors and impact values via pathway enrichment and topology analysis.

4.5. The proteomics analysis of rat liver samples

4.5.1. Protein extraction and digestion

In order to reduce the presence of lipids, proteins were removed utilizing a protein extraction kit (Promega). The extracted proteins were quantified using a BCA Protein Assay Kit (Bio-Rad, USA). Each sample, containing 1g of protein, was heated for 5 min with 24g of total protein, then subjected to electrophoresis on a 16 % stacking gel and an 8 % resolving gel, and stained with Coomassie Brilliant Blue. Overnight digestion with trypsin (Promega) in NH_4HCO_3 at 37 °C followed. After the process of filtration, a total of approximately 2400 μg of protein was collected.

4.5.2. TMT protein labelling and high pH reversed phase fractionation (HPRP)

There were a total of 6 tubes used for all samples. According to the BCA test results, in each group, 100 μg of protein from 4 samples were randomly mixed and allocated to a 1.5 mL centrifuge tube. Thus, each group has two sets of biological replicates(n = 4*2) [42]. Sample preparation and labelling followed the protocol provided by the Pierce TMT® Mass Tagging Kits and Reagents Kit (catalogue number 90113). The high pH reverse-phase fractionation kit comprised a high pH buffer (0.1 % triethylamine) and twelve centrifugal columns with pH-resistant reverse-phase resin. Each column was used in a microcentrifuge to separate 10–100 μg of peptide samples, thereby simplifying sample complexity. Equal amounts of each sample were combined to yield 6 samples. Subsequently, samples were collected and stored on ice.

4.5.3. LC-MS analysis

Each sample received 6 injections for LC-MS/MS analysis,. Phase separation was performed by high-performance liquid chromatography (HPLC) system. Protein analysis was performed using Quality Engineering Plus (QE-Plus) software (Thermo Scientific, Waltham, USA). The initial MS settings included a resolution of 65,000 at m/z 200, a maximum injection time (IT) of 49 ms, and an automatic gain control (AGC) of 1E6. Follow-up MS featured a resolution of 35,000.

4.6. Bioinformatic analysis

Data were analysed using a comprehensive rat database. Bioinformatic data were processed using the Prisma software suite and R, an advanced statistical computing environment. Proteins were screened based on a fold-change ratio exceeding 1.30, with p-values below 0.05 considered statistically significant. Hierarchical clustering analysis facilitated the visualisation of protein expression levels. Enrichment analyses were conducted using R statistical software, targeting the KEGG and GO pathways (Cran Inc., USA). GO annotations were divided into three domains: biological processes (BP), cellular components (CC), and molecular functions (MF). KEGG links known molecular interactions including metabolic pathways, complexes, and biochemical reactions. Cluster analysis determined correlations among differentially expressed proteins based on GO categories, KEGG pathways, and protein domain enrichment.

4.7. RNA preparation, quality control and Real time PCR

Rat tissues were subjected to RNA extraction and isolating using TRIzol reagent (Invitrogen, Beijing, China). Quality control of the

extracted RNA was performed using a Thermo Nanodrop 3000 and an Agilent 2100 Bioanalyzer, along with an Agilent RNA 6000 Nano Kit. High-quality RNA was analysed using microarray technology until it met the specified criteria; when using the Thermo Nanodrop 3000, the A260/A280 ratio was between 1.8 and 2.2. Furthermore, when using the Agilent 2100 bioanalyzer, the RNA Integrity Number (RIN) should be 7 or higher, and the 28S/18S ratio should exceed 1.5. RNA was reverse-transcribed and converted into cDNA with RevertAid First Strand cDNA Synthesis Kit (Thermo Scientific™, K1622). PCR was performed by PCR Master Mix (2X) (Thermo Scientific™, K0171) and StepOne™ RT-PCR system (Applied Biosystems™, 4376357). List of gene-specific primers for RT-PCR analysis is presented in Table S5.

4.8. Data analysis and statistics

The findings were documented in a database and analysed using SPSS 22.0 (SPSS Inc., Chicago, IL, USA). The median and quartile of each set of data were calculated. Pearson's correlations were calculated and for non-normally distributed variables, Kruskal-Wallis assessed differences in serum metabolite levels across time periods, compared to the baseline control before hypoxia exposure. The Dunn test and Bonferroni's multiple comparison post hoc tests were used for pairwise comparisons when the overall test was statistically significant, with the significance level set at $P < 0.05$.

Data availability statement

The mass spectrometry proteomics data were deposited in Figshare with https://doi.org/10.6084/m9.figshare.25376461 (https://figshare.com/s/b428f985a49dac3bc3a3).

However, this study did not report the original codes. Further details necessary to reevaluate the data presented in this work can be obtained from the corresponding author upon enquiry.

Ethics and Consent Statement

The animal study protocol was reviewed and approved by the Ethics Committee of Medical Ethics Committee of Qinghai University School of Medicine with the approval number: 2019-ZJ-876.

Funding

Funding for this work was provided by the National Natural Science Foundation of China (Grant No. 82360333) and the Qinghai Provincial Department of Science and Technology, grant No.2023-ZJ-792.

Code availability

No custom code has been used.

CRediT authorship contribution statement

Jin Xu: Writing – original draft, Methodology, Conceptualization. **Wen-jie Chen:** Writing – original draft, Methodology. **Han-bing Hu:** Data curation. **Zhi-wei Xie:** Data curation. **Dong-ge Zhang:** Investigation. **Jia Zhao:** Data curation. **Jing Xiang:** Formal analysis. **Qi-yu Wei:** Investigation. **Tawni Tidwell:** Writing – review & editing, Investigation. **Olivier Girard:** Conceptualization, Writing – review & editing. **Fu-hai Ma:** Formal analysis. **Zhao-wei Li:** Methodology. **Yan-ming Ren:** Writing – review & editing.

Declaration of competing interest

The authors declare that they have no known competing financial interests or personal relationships that could have appeared to influence the work reported in this paper.

Acknowledgements

We express our gratitude to related staff for providing initial data and their technical assistance. We also acknowledge the contributions of related staff for their work in cell culture. Due to contamination of the culture medium and time, it is regrettably not shown in the article.

Appendix ASupplementary data

Supplementary data to this article can be found online at https://doi.org/10.1016/j.heliyon.2024.e37791.

References

[1] J. Burtscher, R.T. Mallet, M. Burtscher, G.P. Millet, Hypoxia and brain aging: neurodegeneration or neuroprotection? Ageing Res. Rev. 68 (2021) 101343 https://doi.org/10.1016/j.arr.2021.101343.

[2] R.C. Roach, P.H. Hackett, O. Oelz, P. Bärtsch, A.M. Luks, M.J. MacInnis, J.K. Baillie, E. Achatz, E. Albert, J.S. Andrews, J.D. Anholm, M.Z. Ashraf, P. Auerbach, B. Basnyat, B.A. Beidleman, R.R. Berendsen, M.M. Berger, K.E. Bloch, H. Brugger, A. Cogo, R.G. Costa, A. Cumpstey, A. Cymerman, T. Debevec, C. Duncan, D. Dubowitz, A. Fago, M. Furian, M. Gaidica, P. Ganguli, M.P.W. Grocott, D. Hammer, D. Hall, D. Hillebrandt, M.P. Hilty, G. Himashree, B. Honigman, N. Gilbert-Kawai, B. Kayser, L. Keyes, M. Koehle, S. Kohli, A. Kuenzel, B.D. Levine, M. Lichtblau, J. Macdonald, M.B. Maeder, M. Maggiorini, D. Martin, S. Masuyama, J. McCall, S. McIntosh, G. Millet, F. Moraga, C. Mounsey, S.R. Muza, S. Oliver, Q. Pasha, R. Paterson, L. Phillips, A. Pichon, P.A. Pickerodt, M. Pun, M. Rain, D. Rennie, G. Ri-Li, S. Roy, S. Verges, T.B.C. Dos Santos, R.B. Schoene, O.D. Schoch, S. Singh, T. Sooronbaev, C.D. Steinback, M. Stembridge, G. Stewart, T. Stobdan, G. Strapazzon, A.W. Subudhi, E. Swenson, A.A. Roger Thompson, M.T. Van Patot, R. Twomey, S. Ulrich, N. Voituron, D.R. Wagner, S. Wang, J. B. West, M. Wilkes, G. Willmann, M. Yaron, K. Zafren, The Lake Louise AMS Score Consensus Committee, The 2018 lake louise acute mountain sickness score, High Alt. Med. Biol. 19 (2018) 4–6, https://doi.org/10.1089/ham.2017.0164.

[3] J.C. Tremblay, P.N. Ainslie, Global and country-level estimates of human population at high altitude, Proc. Natl. Acad. Sci. USA 118 (2021) e2102463118, https://doi.org/10.1073/pnas.2102463118.

[4] A.J. Murray, J.A. Horscroft, Mitochondrial function at extreme high altitude, J. Physiol. 594 (2016) 1137–1149, https://doi.org/10.1113/JP270079.

[5] J. Wang, S. Liu, Y. Xie, C. Xu, Association analysis of gut microbiota-metabolites-neuroendocrine changes in male rats acute exposure to simulated altitude of 5500 m, Sci. Rep. 13 (2023) 9225, https://doi.org/10.1038/s41598-023-35573-y.

[6] K. Nakanishi, F. Tajima, H. Itoh, Y. Nakata, H. Osada, N. Hama, O. Nakagawa, K. Nakao, T. Kawai, K. Takishima, T. Aurues, T. Ikeda, Changes in atrial natriuretic peptide and brain natriuretic peptide associated with hypobaric hypoxia-induced pulmonary hypertension in rats, Virchows Arch. 439 (2001) 808–817, https://doi.org/10.1007/s004280100454.

[7] M. Luo, T. Li, H. Sang, The role of hypoxia-inducible factor 1α in hepatic lipid metabolism, J. Mol. Med. Berl. Ger. 101 (2023) 487–500, https://doi.org/10.1007/s00109-023-02308-5.

[8] X. Du, R. Zhang, S. Ye, F. Liu, P. Jiang, X. Yu, J. Xu, L. Ma, H. Cao, Y. Shen, F. Lin, Z. Wang, C. Li, Alterations of human plasma proteome profile on adaptation to high-altitude hypobaric hypoxia, J. Proteome Res. (n.d.).

[9] J.L. Sun, L.L. Zhao, H. Wu, Q. Liu, L. Liao, J. Luo, W.Q. Lian, C. Cui, L. Jin, J.D. Ma, M.Z. Li, S. Yang, Acute hypoxia changes the mode of glucose and lipid utilization in the liver of the largemouth bass (Micropterus salmoides), Sci. Total Environ. 713 (2020) 135157, https://doi.org/10.1016/j.scitotenv.2019.135157.

[10] T. Suzuki, Hypoxia and fatty liver, World J. Gastroenterol. 20 (2014) 15087, https://doi.org/10.3748/wjg.v20.i41.15087.

[11] Pooja, V. Sharma, R.N. Meena, K. Ray, U. Panjwani, R. Varshney, N.K. Sethy, TMT-based plasma proteomics reveals dyslipidemia among lowlanders during prolonged stay at high altitudes, Front. Physiol. 12 (2021) 730601, https://doi.org/10.3389/fphys.2021.730601.

[12] Z. Wang, F. Liu, S. Ye, P. Jiang, X. Yu, J. Xu, X. Du, L. Ma, H. Cao, C. Yuan, Y. Shen, F. Lin, R. Zhang, C. Li, Plasma proteome profiling of high-altitude polycythemia using TMT-based quantitative proteomics approach, J. Proteomics 194 (2019) 60–69, https://doi.org/10.1016/j.jprot.2018.12.031.

[13] J. Xu, S. Gao, M. Xin, W. Chen, K. Wang, W. Liu, X. Yan, S. Peng, Y. Ren, Comparative tandem mass tag-based quantitative proteomics analysis of liver against chronic hypoxia: molecular insights into metabolism in rats, High Alt. Med. Biol. 24 (2023) 49–58, https://doi.org/10.1089/ham.2022.0003.

[14] S. Koundal, S. Gandhi, T. Kaur, A. Mazumder, S. Khushu, "Omics" of high altitude biology: a urinary metabolomics biomarker study of rats under hypobaric hypoxia, OMICS A J. Integr. Biol. 19 (2015) 757–765, https://doi.org/10.1089/omi.2015.0155.

[15] I. Sibomana, D.P. Foose, M.L. Raymer, N.V. Reo, J.P. Karl, C.E. Berryman, A.J. Young, S.M. Pasiakos, C.A. Mauzy, Urinary metabolites as predictors of acute mountain sickness severity, Front. Physiol. 12 (2021) 709804, https://doi.org/10.3389/fphys.2021.709804.

[16] J. Gao, M. Zhao, X. Cheng, X. Yue, F. Hao, H. Wang, L. Duan, C. Han, L. Zhu, Metabolomic analysis of human plasma sample after exposed to high altitude and return to sea level, PLoS One 18 (2023) e0282301, https://doi.org/10.1371/journal.pone.0282301.

[17] X.-T. Yu, F. Wang, J.-T. Ding, B. Cai, J.-J. Xing, G.-H. Guo, F. Guo, Tandem mass tag-based serum proteomic profiling revealed diabetic foot ulcer pathogenesis and potential therapeutic targets, Bioengineered 13 (2022) 3171–3182, https://doi.org/10.1080/21655979.2022.2027173.

[18] Y. Xia, X. Huang, L. Mo, C. Wang, W. Fan, H. Huang, TMT-based proteomics analysis of the cerebral cortex of TauT knockout rats, Proteome Sci. 20 (2022) 6, https://doi.org/10.1186/s12953-022-00189-z.

[19] P. Zhao, S. Li, Z. He, F. Zhao, J. Wang, X. Liu, M. Li, J. Hu, Z. Zhao, Y. Luo, Physiology and proteomic basis of lung adaptation to high-altitude hypoxia in Tibetan sheep, Anim. Open Access J. MDPI 12 (2022) 2134, https://doi.org/10.3390/ani12162134.

[20] L.-D. Chen, Z.-W. Huang, Y.-Z. Huang, J.-F. Huang, Z.-P. Zhang, X.-J. Lin, Untargeted metabolomic profiling of liver in a chronic intermittent hypoxia mouse model, Front. Physiol. 12 (2021) 701035, https://doi.org/10.3389/fphys.2021.701035.

[21] J. Yan, K. Song, Z. Bai, R.-L. Ge, WY14643 improves left ventricular myocardial mitochondrial and systolic functions in obese rats under chronic persistent hypoxia via the PPARα pathway, Life Sci. 266 (2021) 118888, https://doi.org/10.1016/j.lfs.2020.118888.

[22] K. Song, Y. Zhang, Q. Ga, Z. Bai, R.-L. Ge, High-altitude chronic hypoxia ameliorates obesity-induced non-alcoholic fatty liver disease in mice by regulating mitochondrial and AMPK signaling, Life Sci. 252 (2020) 117633, https://doi.org/10.1016/j.lfs.2020.117633.

[23] A. Thomas, E. Belaidi, S. Moulin, S. Horman, G.C. van der Zon, B. Viollet, P. Levy, L. Bertrand, J.-L. Pepin, D. Godin-Ribuot, B. Guigas, Chronic intermittent hypoxia impairs insulin sensitivity but improves whole-body glucose tolerance by activating skeletal muscle AMPK, Diabetes 66 (2017) 2942–2951, https://doi.org/10.2337/db17-0186.

[24] J. Krishnan, M. Suter, R. Windak, T. Krebs, A. Felley, C. Montessuit, M. Tokarska-Schlattner, E. Aasum, A. Bogdanova, E. Perriard, J.-C. Perriard, T. Larsen, T. Pedrazzini, W. Krek, Activation of a HIF1α-ppary Axis underlies the integration of glycolytic and lipid anabolic pathways in pathologic cardiac hypertrophy, Cell Metab. 9 (2009) 512–524, https://doi.org/10.1016/j.cmet.2009.05.005.

[25] W. Liao, J. Liu, S. Wang, Z. Xue, F. Zheng, F. Feng, W. Liu, Metabolic profiling reveals that salidroside antagonizes hypoxic injury via modulating energy and lipid metabolism in cardiomyocytes, Biomed. Pharmacother. Biomedecine Pharmacother. 122 (2020) 109700, https://doi.org/10.1016/j.biopha.2019.109700.

[26] G.F. Grabner, H. Xie, M. Schweiger, R. Zechner, Lipolysis: cellular mechanisms for lipid mobilization from fat stores, Nat. Metab. 3 (2021) 1445–1465, https://doi.org/10.1038/s42255-021-00493-6.

[27] M. Prentki, S.R.M. Madiraju, Glycerolipid metabolism and signaling in health and disease, Endocr. Rev. 29 (2008) 647–676, https://doi.org/10.1210/er.2008-0007.

[28] M. Weiszenstein, M. Musutova, A. Plihalova, K. Westlake, M. Elkalaf, M. Koc, A. Prochazka, J. Pala, S. Gulati, J. Trnka, J. Polak, Adipogenesis, lipogenesis and lipolysis is stimulated by mild but not severe hypoxia in 3T3-L1 cells, Biochem. Biophys. Res. Commun. 478 (2016) 727–732, https://doi.org/10.1016/j.bbrc.2016.08.015.

[29] J.T. Noe, R.A. Mitchell, Tricarboxylic acid cycle metabolites in the control of macrophage activation and effector phenotypes, J. Leukoc. Biol. 106 (2019) 359–367, https://doi.org/10.1002/JLB.3RU1218-496R.

[30] B. Li, Y. Hong, Y. Gu, S. Ye, K. Hu, J. Yao, K. Ding, A. Zhao, W. Jia, H. Li, Functional metabolomics reveals that Astragalus polysaccharides improve lipids metabolism through microbial metabolite 2-hydroxybutyric acid in obese mice, Engineering 9 (2022) 111–122, https://doi.org/10.1016/j.eng.2020.05.023.

[31] A. Wiecikowski, K.M.D.S. Cabral, M. da S. Almeida, R.S. Carvalho, Ligand-free method to produce the anti-angiogenic recombinant Galectin-3 carbohydrate recognition domain, Protein Expr. Purif. 144 (2018) 19–24, https://doi.org/10.1016/j.pep.2017.11.006.

[32] Y.G. Jeon, Y.Y. Kim, G. Lee, J.B. Kim, Physiological and pathological roles of lipogenesis, Nat. Metab. 5 (2023) 735–759, https://doi.org/10.1038/s42255-023-00786-y.

[33] Z.E. Amine, J.-F. Mauger, P. Imbeault, CYP1A1, VEGFA and adipokine responses of human adipocytes Co-exposed to PCB126 and hypoxia, Cells 11 (2022) 2282, https://doi.org/10.3390/cells11152282.

[34] C. Glaser, J. Heinrich, B. Koletzko, Role of FADS1 and FADS2 polymorphisms in polyunsaturated fatty acid metabolism, Metabolism 59 (2010) 993–999, https://doi.org/10.1016/j.metabol.2009.10.022.
[35] A.K. Singh, B. Aryal, B. Chaube, N. Rotllan, L. Varela, T.L. Horvath, Y. Suárez, C. Fernández-Hernando, Brown adipose tissue derived ANGPTL4 controls glucose and lipid metabolism and regulates thermogenesis, Mol. Metab. 11 (2018) 59–69, https://doi.org/10.1016/j.molmet.2018.03.011.
[36] I. Mylonis, G. Simos, E. Paraskeva, Hypoxia-inducible factors and the regulation of lipid metabolism, Cells 8 (2019) 214, https://doi.org/10.3390/cells8030214.
[37] F.J. Gonzalez, C. Xie, C. Jiang, The role of hypoxia-inducible factors in metabolic diseases, Nat. Rev. Endocrinol. 15 (2019) 21–32, https://doi.org/10.1038/s41574-018-0096-z.
[38] M.A. De La Rosa Rodriguez, L. Deng, A. Gemmink, M. Van Weeghel, M.L. Aoun, C. Warnecke, R. Singh, J.W. Borst, S. Kersten, Hypoxia-inducible lipid droplet-associated induces DGAT1 and promotes lipid storage in hepatocytes, Mol. Metab. 47 (2021) 101168, https://doi.org/10.1016/j.molmet.2021.101168.
[39] K. Belosludtsev, M. Dubinin, E. Talanov, V. Starinets, K. Tenkov, N. Zakharova, N. Belosludtseva, Transport of Ca2+ and Ca2+-dependent permeability transition in the liver and heart mitochondria of rats with different tolerance to acute hypoxia, Biomolecules 10 (2020) 114, https://doi.org/10.3390/biom10010114.
[40] G.D. Mironova, L.L. Pavlik, Y.I. Kirova, N.V. Belosludtseva, A.A. Mosentsov, N.V. Khmil, E.L. Germanova, L.D. Lukyanova, Effect of hypoxia on mitochondrial enzymes and ultrastructure in the brain cortex of rats with different tolerance to oxygen shortage, J. Bioenerg. Biomembr. 51 (2019) 329–340, https://doi.org/10.1007/s10863-019-09806-7.
[41] G.D. Mironova, M.I. Shigaeva, E.N. Gritsenko, S.V. Murzaeva, O.S. Gorbacheva, E.L. Germanova, L.D. Lukyanova, Functioning of the mitochondrial ATP-dependent potassium channel in rats varying in their resistance to hypoxia. Involvement of the channel in the process of animal's adaptation to hypoxia, J. Bioenerg. Biomembr. 42 (2010) 473–481, https://doi.org/10.1007/s10863-010-9316-5.
[42] D. Xu, X. Zhu, J. Ren, S. Huang, Z. Xiao, H. Jiang, Y. Tan, Quantitative proteomic analysis of cervical cancer based on TMT-labeled quantitative proteomics, J. Proteomics 252 (2022) 104453, https://doi.org/10.1016/j.jprot.2021.104453.